Received: 27 January 2026 | *Revised:* 2 March 2026 | *Accepted:* 6 March 2026 | *Vol. 2 | Issue 1| June 2026*
e ISSN: 3105-2169

International Journal of Mechatronics, Robotics, and Artificial Intelligence
Original Article

Robust Feedback Linearization Based PSO Algorithm for Overhead Crane System

Jasim M. Khalaf *[1], Ahmad Al-Talabi[2], Ali Mary[1]
[1] Department of Mechatronics Engineering, Khwarizmi College of Engineering, University of Baghdad, Baghdad, Iraq
[2] Department of Medical Instrumentation Techniques, College of Engineering and Information Technology, AlShaab University, Baghdad, Iraq

Correspondence
*Jasim Mohammed Khalaf
Department of Mechatronics Engineering, Khwarizmi College of Engineering, University of Baghdad, Baghdad 10071, Iraq
Email: jassem.khalaf2402m@kecbu.uobaghdad.edu.iq

Abstract
Overhead crane systems are found in many industrial environments; however, controlling their motion in the presence of nonlinear and underactuated dynamics considers as a big challenge. To address this, a nonlinear control method proposed to enable the trolley to track the desired trajectory and quickly eliminate swing. First, feedback linearization is applied to the crane dynamics. Next, an energy-based compensation is implemented to ensure the boundedness of the system trajectories. Then, Particle Swarm Optimization (PSO) is utilized to optimally tune the controller parameters. The optimization relies on a multi-objective cost function formulated to simultaneously minimize steady-state error and overshoot, while improving robustness against model uncertainties and external disturbances. Finally, the robustness and validity of the proposed control method are demonstrated through the simulation of an underactuated crane system in several cases, including reference tracking, robustness against system uncertainty and external disturbances. Simulation results illustrated that the presented control method has minimum rise time, settling time with respect other control methods with zero steady state error.

Keywords
Overhead Crane Systems, Nonlinear Dynamics, Particle Swarm Optimization (PSO), Payload Swing Suppression

I. INTRODUCTION

When being utilized in a modern industrial environment, an overhead crane is one of the essential systems used today, providing a fairly inexpensive, efficient, and safe way to handle heavy loads with multiple degrees of freedom. However, due to under actuation, these systems exhibit complex nonlinear dynamics, making them difficult to control, since control inputs cannot directly command all motion axes. Consequently, more advanced control solutions are required to stabilize the system while achieving precise and accurate motion control. While traditional Proportional–Integral–Derivative (PID) control strategies remain highly useful due to their simplicity and reliable overall performance as a baseline approach, more advanced techniques, such as Particle Swarm Optimization (PSO) combined with Simulated Annealing (SA), can significantly improve swing reduction and system stability [1][2]. Improving PID controllers with optimization approaches and evolutionary algorithms such as genetic algorithms and the Bees Algorithm, have also shown reduced overshoot and better settling behavior [3]. Introduced in the 1960s by Zadeh, Fuzzy Logic Control (FLC) allows tolerance to modeling abstractions and has been applied to address anti-swing problems in overhead crane system [4][5]. More recently, hybrid fuzzy control approaches, like Takagi-Sugeno (TS) fuzzy controllers, have improved performance in dynamic crane situations [6][7]. Also, neural network approaches have been used extensively and have demonstrated strong performance due to their flexibility. In particular, predictive neural controllers can better reject disturbances [8] and neural compensation method can effectively suppress sway in double-pendulum crane systems [9][10]. Beyond single approaches, there are also composite approaches that combine multiple control paradigms that are becoming popular. One approach that combines both adaptive input shaping and application of a dual-loop PD feedback controller achieved a large amount of sway reduction and system robustness demonstrated in double-pendulum systems [11]. Another approach that uses disturbance observers and energy storage functions also increased the stability of two-dimensional crane models [12]. An additional advanced adaptive control approach addressed to advanced load shape-specification to suppress swing in a four-degrees-of-freedom crane robot can operate quite well even without the need for pendulum angle feedback [13]. All the approaches highlight fundamental challenges related to payload swing, disturbances and uncertainties while improving systems' flexibility, operational efficiency, and maintaining robustness in the crane systems examined. Although, there are progress

in control of overhead crane system, they are suffering from many weaknesses. PID and LQR (Linear Quadratic Regulator) controllers are poor robustness to payload variations while fuzzy logic control suffering from complexity of rule design and risk of instability. Sliding mode control has the problem of chattering while feedback linearization requires accurate modeling of the dynamic system. Unlike previous control methods that applied feedback linearization without robustness enhancement or use PSO to tune linear PID structures, the proposed method improves the feedback linearization by adding robust term and use PSO to get optimal control gains. This hybrid approach preserves the nonlinear cancelation capability of feedback linearization while improving robustness against payload variations and external disturbances through optimal gain selection. The stability of this combination has been approved by Lyapunov theorem. The remainder of this manuscript is organized as follows: The dynamic equations of motion of the overhead crane system are presented in Section 2. Section 3 describes the proposed control method along with the associated optimization algorithm. The simulation results are discussed in Section 4 to demonstrate the effectiveness of the proposed approach. The paper is concluded in Section 5 by summarizing the main findings and suggesting directions for future work.

II. DYNAMIC EQUATIONS OF MOTION OF AN OVERHEAD CRANE SYSTEM

The overhead crane system is dynamic and can be systematically modeled using the Lagrangian formulation, a somewhat classical method for describing complex mechanical systems. The equations of motion are derived from the free-body diagrams using the Lagrangian equations with appropriate generalized coordinates [10]. The main advantage of using this model is not only capturing both the kinetic and potential energy contributions to the system but also providing a more systematic and functional way to develop nonlinear dynamic models more accurately and consistently [10]. Fig.1 shows the free-body diagram of the overhead crane system.

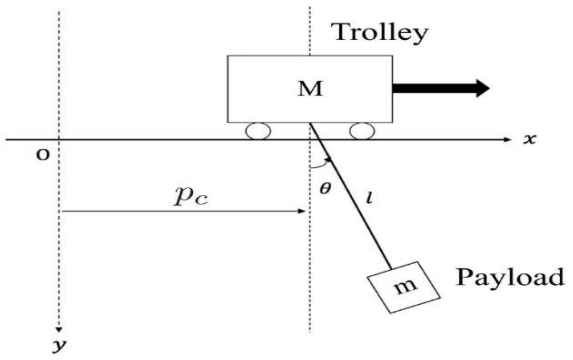

Fig.1. Overhead crane system [11]

The dynamic equations that describe the motion of the overhead crane system are given by:

Trolly (horizontal motion):

$$(M+m)\ddot{x} + mL\ddot{\theta}\cos\theta - mL\dot{\theta}^2\sin\theta = U \quad (1)$$

Payload (swing motion):

$$\ddot{x}\cos\theta + L\ddot{\theta} + g\sin\theta = 0 \quad (2)$$

Where:
x: horizontal position of the trolley
θ: payload swing angle
M: mass of the trolley
m: mass of the payload,
L : length of the hoisting cable (assumed rigid and massless),
g : Gravitational acceleration
θ : Pendulum angle
U: External force applied to the trolley
$\dot{\theta}$: Payload angular velocity
$\ddot{\theta}$: Payload angular acceleration
$\ddot{x}$: Trolley acceleration.

III. PROPOSED CONTROL METHOD AND OPTIMIZATION ALGORITHM

This section describes a composite control approach developed for underactuated overhead cranes system that combines feedback linearization with energy-based compensation, along with the PSO algorithm to optimize the controller parameters. This approach provides fast and low-sway motion for trajectories subject to input limitations. The system is designed to achieve two objectives: (i) minimizing the swing angle while accurately positioning the trolley and limiting the control effort, and (ii) providing fast ring-down (i.e., no visible oscillations) within a specified time frame. The semi-composite model integrates model-based inversion for trajectory shaping with energy dissipation to manage sway, making such composite structures well suited for crane systems. The proposed control law can be expressed as follows:

$$U = U_f + U_e \quad (3)$$

Where U_f refers to the Feedback-linearization term and U_e denotes the Energy-based compensation term. To drive these terms, define the output tracking error y as follows:

$$y = -\theta + c(x_d - x) \qquad c > 0 \quad (4)$$

where x_d referes to the desired cart position. Rewrite the dynamic model as follows:

$$\begin{aligned} \ddot{x} &= F_x(\theta, \dot{\theta}) + G_x(\theta)U \\ \ddot{\theta} &= F_\theta(\theta, \dot{\theta}) + G_\theta(\theta)U \end{aligned} \quad (5)$$

where $F_x(\cdot)$and $F_\theta(\cdot)$represent the nonlinear dynamics of the system, and $G_x(\cdot)$, $G_\theta(\cdot)$denote the corresponding input gain functions.

$$F_x = \frac{mg\sin\theta\cos\theta + mL\dot{\theta}^2\sin\theta}{D} \quad (6)$$

$$G_x = \frac{1}{D} \quad (7)$$

$$F_\theta = \frac{-mL\dot{\theta}^2\sin\theta\cos\theta - g\sin\theta(M+m)}{LD} \quad (8)$$

$$G_\theta = \frac{-\cos\theta}{LD} \quad (9)$$

Now, determine the first and second of the output tracking error

$$\dot{y} = -\dot{\theta} + c(\dot{x}_d - \dot{x}) \quad (10)$$

$$\ddot{y} = c\ddot{x}_d - (F + GU) \quad (11)$$

Where

$$F = F_\theta + cF_x \quad (12)$$

$$G = G_\theta + cG_x \tag{13}$$

then

$$U_f = \frac{c\ddot{x}_d + k_{d2}\dot{y} + k_{p2}y - F}{G} \tag{14}$$

with gains $k_{p2} > 0, k_{d2} > 0$

This yields the linear output dynamics

$\ddot{y} + k_{d2}\dot{y} + k_{p2}y = 0 \implies y(t) \to 0$ exponentially.

This term can ensure the robustness of the proposed controller. Thus, compensation robust term will be added to the presented control low and Lyapunov theorem used has been used to design this term. The proposed compensation expressed as follows:

$$U_e = -\gamma\left[\sigma_1 G_\theta(\theta)\theta + G_\theta(\theta)\dot{\theta} - \delta\sigma_2 G_x(\theta)(x_d - x) - \delta G_x(\theta)\dot{x}\right] - k_{p1}G_\theta(\theta)\theta - k_{d1}G_\theta(\theta)\dot{\theta} \tag{15}$$

where $\gamma, k_{p1}, k_{d1} > 0$ are positive control gains, and σ_1, σ_2, and δ are design parameters

B. Lyapunov stability

The stability of the proposed control method for the underactuated overhead crane system is verified using the Lyapunov stability theorem. The Lyapunov candidate function is defined as follows:

$$V = \frac{1}{2}\dot{\theta}^2 + \frac{1}{2}k_{p1}\theta^2 + \epsilon_1\theta\dot{\theta} + \vartheta(\theta) + \delta\left[\frac{1}{2}\dot{x}^2 + \frac{1}{2}k_{p2}x^2 + \epsilon_2 x\dot{x}\right] \tag{16}$$

Taking the time derivative of V:

$$\dot{V} = \epsilon_1\dot{\theta}^2 + k_{p1}\theta\dot{\theta} + \left[\dot{\theta} + \epsilon_1\theta\right]\left(F_1 + G_1\tau_f\right) + \phi(\theta)\dot{\theta} + \left[\epsilon_1 G_1\theta + G_1\dot{\theta} - \delta\epsilon_2 G_x - \delta G\dot{x}\right]U_e - \delta\begin{bmatrix}x\\ \dot{x}\end{bmatrix}^T\begin{bmatrix}\epsilon_2 k_{p2} & \frac{1}{2}\epsilon_2 k_{d2}\\ \frac{1}{2}\epsilon_2 k_{d2} & k_{d2} - \epsilon_2\end{bmatrix}\begin{bmatrix}x\\ \dot{x}\end{bmatrix} \tag{17}$$

The control input τ_e is defined as: $\tau_e = -\gamma\left[\epsilon_1 G_1\theta + G_1\dot{\theta} - \delta\epsilon_2 G_x - \delta G\dot{x}\right] - k_{p1}G_1\theta - k_{d1}G_1\dot{\theta}$ (18)

Substituting (19) into (18) gives:

$$\dot{V} = -\epsilon_1 k_{p1}G_1^2\theta^2 - \left(\epsilon_1 k_{d1}G_1^2 + k_{p1}G_1^2 - k_{p1}\right)\theta\dot{\theta} - (k_{d1}G_1^2 - \epsilon_1)\dot{\theta}^2 + \phi(\theta)\dot{\theta} + \delta[\epsilon_1 G_x + G\dot{x}]\left(k_{p1}G_1\theta + k_{d1}G_1\dot{\theta}\right) + \left[\dot{\theta} + \epsilon_1\theta\right]\left(F_1 + G_1\tau_f\right) - \gamma\left[\epsilon_1 G_1\theta + G_1\dot{\theta} - \delta\epsilon_2 G_x - \delta G\dot{x}\right]^2 - \delta\begin{bmatrix}x\\ \dot{x}\end{bmatrix}^T\begin{bmatrix}\epsilon_2 k_{p2} & \frac{1}{2}\epsilon_2 k_{d2}\\ \frac{1}{2}\epsilon_2 k_{d2} & k_{d2} - \epsilon_2\end{bmatrix}\begin{bmatrix}x\\ \dot{x}\end{bmatrix} \tag{19}$$

By choosing the scalar function

$$\phi(\theta)\dot{\theta} = \left[\epsilon_1 k_{d1}G_1^2 + k_{p1}G_1^2 - k_{p1}\right]\theta\dot{\theta} \tag{20}$$

and substituting it into (20), the Lyapunov function derivative becomes:

$$\dot{V} = -\begin{bmatrix}\theta\\ \dot{\theta}\end{bmatrix}^T\begin{bmatrix}\epsilon_1 k_{p1}G_1^2 & 0\\ 0 & k_{d1}G_1^2 - \epsilon_1\end{bmatrix}\begin{bmatrix}\theta\\ \dot{\theta}\end{bmatrix} - \delta\begin{bmatrix}x\\ \dot{x}\end{bmatrix}^T\begin{bmatrix}\epsilon_2 k_{p2} & \frac{1}{2}\epsilon_2 k_{d2}\\ \frac{1}{2}\epsilon_2 k_{d2} & k_{d2} - \epsilon_2\end{bmatrix}\begin{bmatrix}x\\ \dot{x}\end{bmatrix} - \gamma P^2 + \Delta \tag{21}$$

where the auxiliary terms $P$and Δ are defined as:

$$P = \epsilon_1 G_\theta(\theta)\,\theta + G_\theta(\theta)\,\dot{\theta} - \delta\epsilon_2 G_x(\theta) - \delta G_x(\theta)\,\dot{x} \tag{22}$$

$$\Delta = \left(\dot{\theta} + \epsilon_1\theta\right)\left(F_\theta(\theta,\dot{\theta}) + G_\theta(\theta)\,U_f\right) \tag{23}$$

where ϵ_1, ϵ_2, and $\delta$are positive design constants.

By selecting the constant

$$\alpha \le \epsilon_1 k_{d1}G_1^2 + k_{p1}G_1^2 \tag{24}$$

and considering

$$\epsilon_1 < \sqrt{\alpha} \le \sqrt{\epsilon_1 k_{d1}G_1^2 + k_{p1}G_1^2} \tag{25}$$

the positive definiteness of V is guaranteed if the following inequalities are satisfied:

$$\epsilon_1 < \sqrt{\epsilon_1 k_{d1}G_1^2 + k_{p1}G_1^2} \tag{26}$$

and also

$$\epsilon_1 < \sqrt{k_{p1}G_1^2} \tag{27}$$

When evaluating the simplified stability condition versus non-linear bounds that are convoluted in structure and often impose more constraints in practice, inserting the definition of ϕ(θ) into the derivative of V to show the Lyapunov function remains positive definite (to be more explicit, radially unbounded) guarantees that both variables, x (the cart position) and θ (payload angle), will asymptotically converge towards zero. The implication of this statement is that we will guarantee asymptotic stability of the underactuated overhead crane system using the proposed composite control law.

System Stability is ensured for $\epsilon_1 < \sqrt{k_{p1}G_1^2}$

C. Multi-objective PSO tuning

A multi-objective optimization technique has been applied to achieve many objective functions with the following performance index:

$$J(p) = \int_0^T (w_\theta\theta^2(t) + w_x(x(t) - x_d)^2 + w_{ud}u^2(t))dt + w_{\text{term}}\,(\theta^2(T) + (x(T) - x_d)^2) + \int_6^7 \left(w_{\text{ring},\,67}\theta^2(t) + w_{\dot{\theta}}\dot{\theta}^2(t) + w_{x,\,\text{tight}}\,(x(t) - x_d)^2\right)dt + \int_7^T w_{\text{ring,tail}}\,\theta^2(t)dt \tag{28}$$

A Particle Swarm Optimization technique is utilized to find appropriate values for the proposed controller parameters through minimization of the multi-objective performance

index specified previously by equation (28). Each particle of this optimization represents a potential solution vector comprising the controller parameters that need to be adjusted and the PSO controller tuning algorithm begins by randomly generating the initial particle positions within the confines of pre-defined lower and upper bounds. For each particle, the crane model obtained is run through a simulation over a time horizon (T) and the corresponding objective function J(p) is computed based on weighted tracking errors, suppression of swing, control effort, terminal penalties, swing down behavior given (tr) penalty for peak swing angle and use of actuator saturation. The (pbest) position of each particle is updated as is the global best (gbest) position of the swarm based upon the values generated by the fitness evaluations. After having updated both the p best and g best values, the velocity and position of each individual particle are recalculated using the basic PSO velocity and position update equations that are determined using inertia weight, cognitive coefficient, and social coefficient. The above steps are continually performed until either the maximum number of iterations is reached or the objective function has converged. The final global best solution is chosen to represent the optimal controller parameter values. The configuration of the simulation is shown in summary format in three separate tables. Table I lists the weighting factors used in the multi-objective cost function which describe how important each objective is to the entire project, including but not limited to tracking accuracy, swing attenuation, control energy, terminal constraints and post-settling oscillation penalties. Table II describes the parameters for the PSO algorithm such as swarm size, max number of iterations, inertia weight, the coefficients for cognitive and social acceleration. The third table shows all of the values for the proposed controller parameters after convergence of the PSO algorithm. These three sets of tables provide transparency and reproducibility of the optimization and simulation processes.

VI. SIMULATION RESULTS

The PID, SMC (Sliding-Mode Control), and proposed composite controllers will all be independently tested using the same simulation environment to provide an objective evaluation of each control strategy's performance by using identical system parameters, disturbance conditions, duration, and reference trajectories. Each controller was tuned exactly the same as per standard design procedure in order to achieve maximum performance under uniform conditions in this experiment. Therefore, any difference in performance metrics is strictly due to the different structure of each control strategy. The system parameters are summarized as follows: m=1kg, M=2kg, L=1m and g=9.81m/s^2, while the weighting factors used in the control design are summarized in Table I. The values of these factors selected after trial and error until get good results. Table II lists the parameters setting of the PSO algorithm. In this study, the PSO algorithm was used to estimate the optimal controller parameters by minimizing the cost function defined by equation (28). The resulting optimal parameter values of the proposed controller are given in Table III. In this simulation, three scenarios were considered: reference tracking, rejection of external disturbances and robustness against system uncertainties. All simulations were conducted using MATLAB/Simulink. The nonlinear crane model was implemented using differential equations, and the controllers were evaluated under identical simulation conditions.

TABLE I.
THE WEIGHT FACTOR USED IN SIMULATION

Term	Description	Weight factor
$\boldsymbol{w_\theta}$	Payload angle tracking error	280
$\boldsymbol{w_x}$	Cart position tracking error	60
$\boldsymbol{w_{ud}}$	Control effort (input energy)	0.0045
$\boldsymbol{w}_{\text{term}}$	Terminal position and angle error	260
$\boldsymbol{w}_{\text{ring, 67}}$	Swing penalty between 6-7 s	2200
$\boldsymbol{w}_{\text{ring,tail}}$	Swing penalty after 6 s	900
$\boldsymbol{w}_{x,\text{ tight}}$	Tight position constraint (6-7 s)	900
$\boldsymbol{w_{\dot\theta}}$	Angular velocity penalty	150

TABLE II.
PSO ALGORITHM PARAMETERS

Parameter	Description	Value
n_{Pop}	Number of particles in the swarm	35
Max_{It}	Maximum number of iterations	70
w	Inertia weight (initial value)	0.72
w_{damp}	Inertia damping ratio	0.985
c_1	Cognitive coefficient	1.6
c_2	Social coefficient	1.6
$V_{\max}$	Maximum particle velocity (20% of search range)	$0.20 \times$ (VarMax - VarMin)
$V_{\min}$	Minimum particle velocity	$-V_{\max}$
Random seed	Random number generator seed for (reproducibility)	4

TABLE III.
OPTIMAL VALUES OF PROPOSED CONTROLLER

Parameters	values
c	3.4173
k_{p1}	423.412
k_d1	118.253
k_{p2}	10.063
k_{d2}	10.006
γ	17.165

A. Step Reference Tracking

A step input function used as reference input has been used to compare the reference tracking of the three controllers. The cart position shown in Fig.2 convergence rapidly to a unit step reference with minimal overshoot and a settling time of approximately 4-5 seconds, while the payload angle, as shown in Fig.3, is simultaneously damped with reduced oscillation within the same time interval. This behavior confirms that the composite controller achieves both fast positioning and effective swing reduction. The SMC is defined as $U = -K\theta -$

$K\dot{\theta} - Kx \cdot \tanh(S)$, where the sliding surface is given by $S=e^{\cdot}+\lambda xe$. The SMC parameters $K\theta$, $K\dot{\theta}, Kx$ *and* λx were optimized using the PSO algorithm and set to (0.1,0.1,8,0.5), respectively. The response of the SMC and PID controllers for the cart position and payload angle are shown in Figs.2 and 3, respectively. Compared to the PID controller, the SMC exhibits slower convergence to the desired cart position; however, it offers greater robustness with reduced oscillatory behavior. In addition, the payload swing under SMC decays more rapidly and reaches lower amplitudes than under PID controller, indicating improved ability to nonlinear effects. The PID controller was tuned using the pole placement method with gains Kp=30, Ki=30, Kd= 24.7642 for the payload angle and Kp=2.4378, Ki=0.1, Kd= 7.0626 for the cart position. While the PID controller provides faster rise time and initial convergence, it exhibits large overshoot and slower attenuation of residual oscillations. Overall, the composite controller achieves the most balance performance, the SMC demonstrates strong robustness and the PID offers rapid response at the cost of reduced stability.

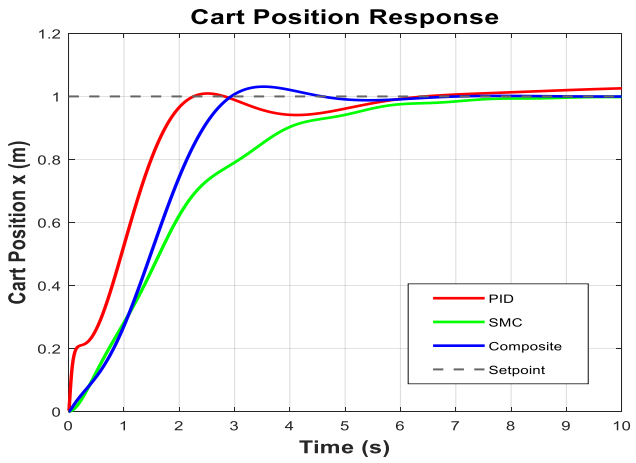

Fig.2. Step response for cart position

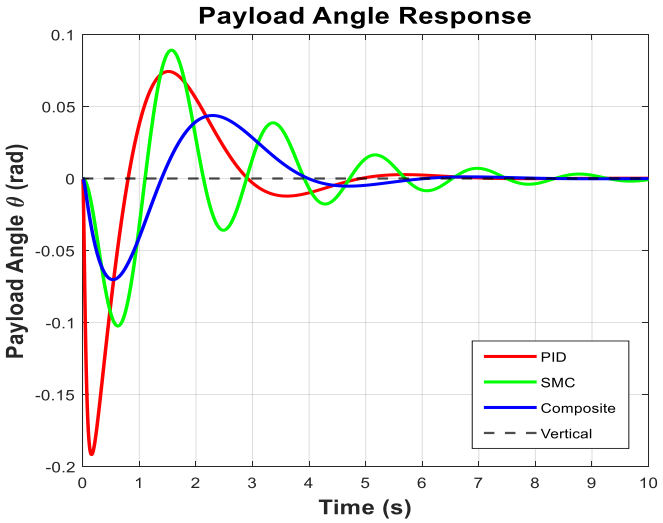

Fig.3. Step response for payload angle (θ)

B. Ramp Reference Tracking

To evaluate the continuous-motion tracking capability of the crane system, a ramp reference input was applied to the cart position. The desired trajectory was defined as $x_d(t) = at$, where the ramp slope was selected as $a = 0.9$, corresponding to constant-velocity motion. For the Composite controller, PSO is used to optimize a multi-objective cost function that considers the swing of a payload, the error of the payload, and the effort used in control.$c = 3.4173$, $k_{p1} = 400$, $k_{d1} = 108.$, $\gamma = 18$, $\delta = 0.33$, $\sigma_1 = 0.21$, and $\sigma_2 = 0.13$, These parameters were selected to achieve a balance between ramp tracking accuracy and payload swing suppression while avoiding excessive control effort. The simulation results indicate that all controllers are capable of tracking the ramp reference with acceptable performance. The Composite controller demonstrates superior tracking accuracy, closely following the desired trajectory with reduced steady-state error compared to PID and SMC strategies. The PID controller exhibits a small tracking lag, while the SMC controller shows slower convergence in the initial phase due to switching behavior and control saturation effects. In terms of payload angle response, the Composite controller achieves faster oscillation damping and reduced swing amplitude. Although the SMC controller produces a larger transient oscillation at the beginning of motion, it stabilizes the payload angle within a short duration. Overall, the results confirm that, under the specified system parameters and ramp input conditions, the Composite controller provides improved trajectory tracking performance while effectively minimizing payload oscillations. evident from the cart position and payload angle in Figs.4 and 5 and the Table IV show the time-domain performance under ramp reference input.

C. Disturbance Rejection

The ability of the three controllers to reject disturbances was evaluated by introducing an external disturbance of amplitude 1 at 6.5 second, as demonstrated in Figs.6 and 7. From these figures, it is shown that with the composite controller, the cart position response remained stable and closely followed the reference despite the disturbance, while the payload oscillations decayed rapidly within a short time. This demonstrates that the composite controller provides accurate trolley positioning while effectively suppressing payload swing under external disturbances. In comparison, the SMC exhibited greater robustness than the PID controller. As illustrated in Figs.6 and 7, the disturbance-induced oscillations under SMC control were smaller in amplitude and decayed faster than those observed with the PID controller. Although the cart position response of the PID controller, as seen in Fig.6, showed a faster initial correction following the disturbances, this improvement came at the cost of larger overshoot and persistent payload oscillations as seen in Fig.7, thereby reducing its overall effectiveness under system uncertainty. Overall, the disturbance rejection results indicate that the composite controller offers the most balanced in performance, the SMC controller provides the highest robustness against nonlinearities and disturbances, and PID achieves the fastest convergence but suffers from excessive overshoot and poor damping effect on payload oscillations.

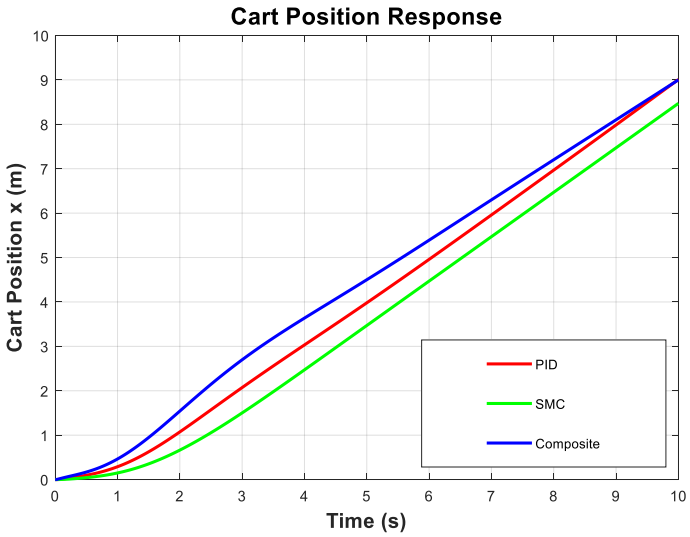

Fig .4. Ramp response for cart position

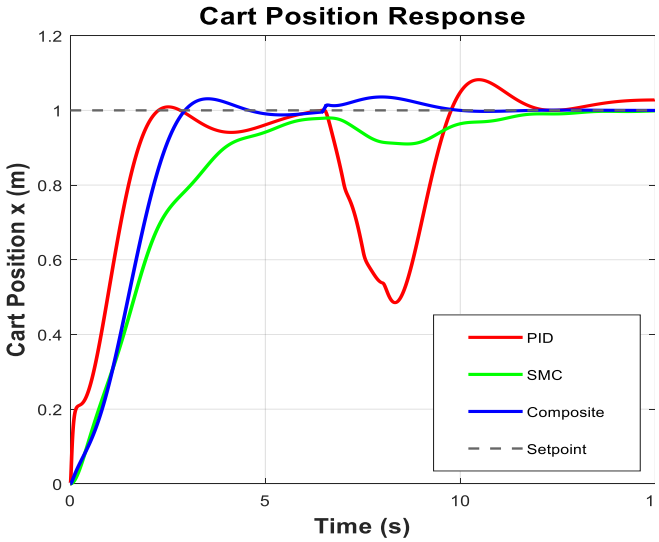

Fig .6. Response of cart position (x) for disturbance

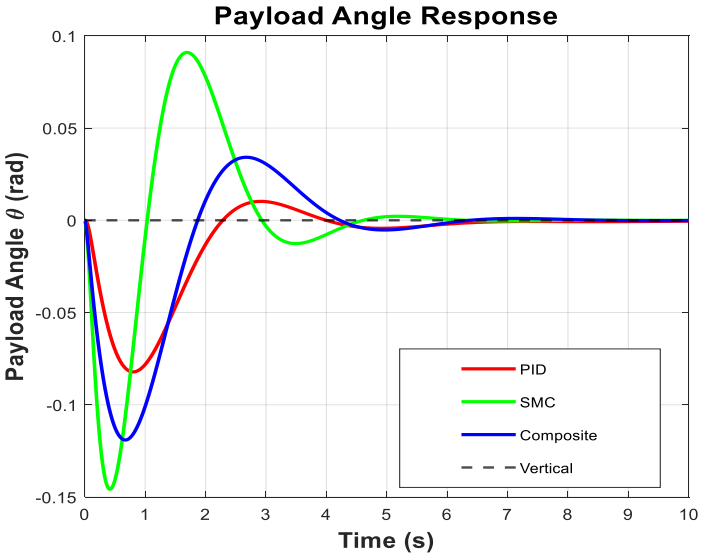

Fig .5. Ramp response for payload angle (θ)

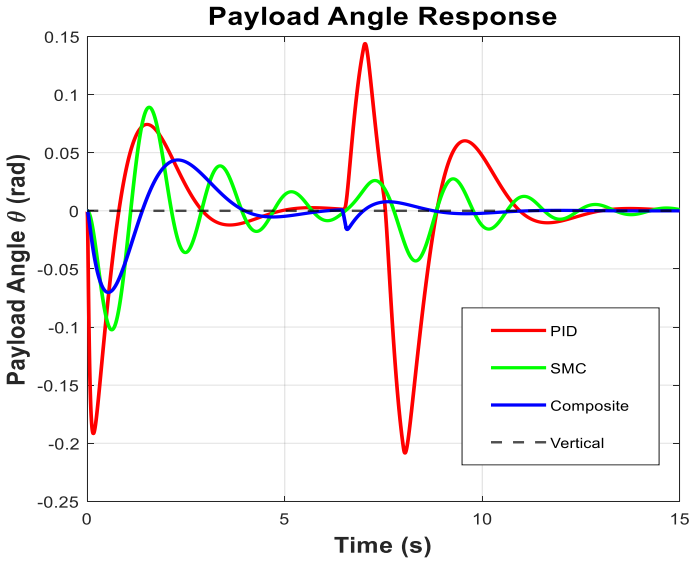

Fig .7. Response of payload angle (θ) for disturbance

TABLE IV.
TIME-DOMAIN PERFORMANCE UNDER RAMP REFERENCE INPUT

Controller	Rise Time (s)	Settling Time (s)	Overshoot (%)	Maximum Swing Angle (rad)
PID	2.5	4.5	5	0.085
SMC	3.0	5.0	25	0.145
Composite	2.0	3.5	12	0.120

D. System Uncertainty

To examine the performance of the controller under uncertainty, the parameters of the crane system were modified to a cart mass of M=2.6kg, a payload mass of m=1.3kg and a cable length of l=1.4m, which introduced additional nonlinear dynamics and increased sensitivity to parameter changes. The response of the composite controller under uncertainty is shown in Figs.8 and 9. The composite control scheme provides a precise tracking of the cart position, as shown in Fig.8, with minimal overshoot, while the payload swing is effectively rejected and damped, as shown in Fig.9. Overall, the optimization-based design demonstrates robustness under uncertain conditions, with variations in nominal system parameters explicitly considered. Figs.8 and 9 also show the SMC and PID controllers' responses under the same uncertainty conditions. The SMC response exhibits good robustness compared to the other controllers, although its dynamics are slower; but the reference was evident from the cart position in Fig.8, where the initial position was reliable and converging in position and response. The swing in the

payload was well damped quickly and reliably within constraints in Fig.9. Finally, the PID controller converged quickly, but under uncertainty, this caused performance degradation, which then resulted in an increase in overshoot and oscillatory nature. A comparison of related control methods and algorithms is summarized in Table V.

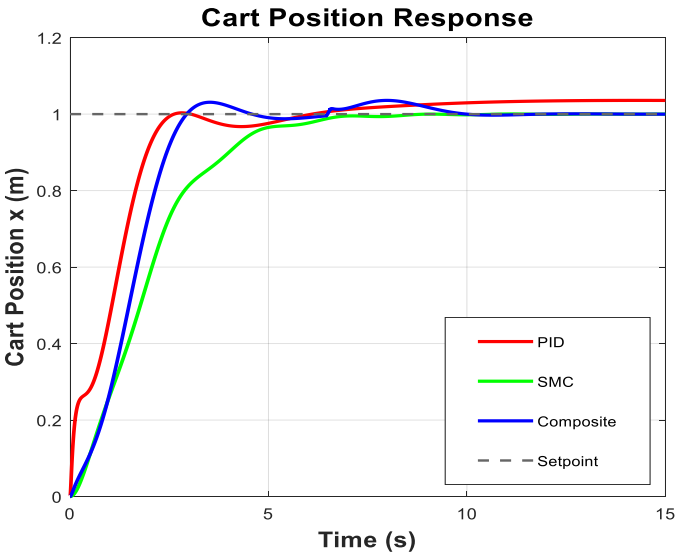

Fig.8. Response of cart position (x) for uncertainty.

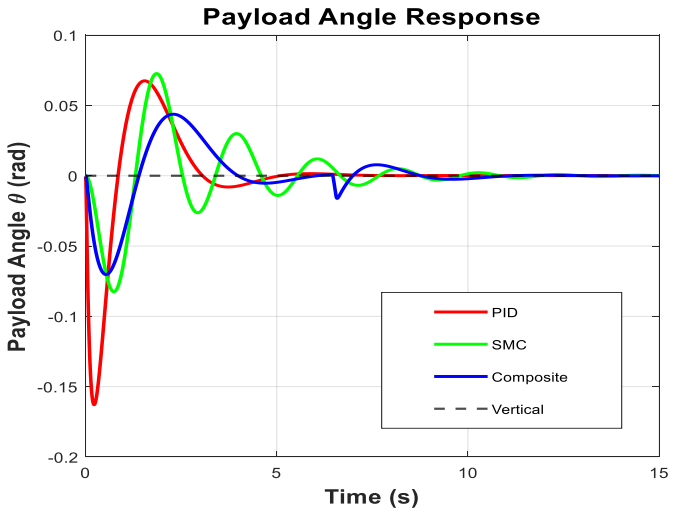

Fig .9. Response of payload angle (θ) for uncertainty

TABLE V.
COMPARISON OF RELATED CONTROL METHODS FOR OVERHEAD CRANE SYSTEMS

Method	Advantages	Limitations
PID-based control	Simple structure and easy implementation; low computational cost	Limited robustness to nonlinearities and disturbances; performance degrades under varying payload conditions
Sliding Mode Control (SMC)	Strong robustness against uncertainties and external disturbances; effective swing suppression	Chattering phenomenon; high control effort and increased implementation complexity
Nonlinear /Composite control	Enhanced tracking performance and swing reduction	Increased controller complexity; lack of systematic tuning methods
PSO-tuned Composite Control	Systematic parameter optimization; improved tracking and swing suppression under identical conditions	Simulation-based validation; experimental implementation not yet considered

VI. Conclusion

This study presented a comprehensive nonlinear simulation of an underactuated overhead crane system to evaluate the performance and robustness of three control strategies: a composite controller, SMC and a PID controller. Through step reference tracking experiments, the composite controller demonstrated the most balanced performance. It achieved rapid and precise cart positioning with minimal overshoot while effectively suppressing payload oscillations. In comparison, the PID controller delivered faster initial convergence but exhibited higher overshoot and slower damping of residual oscillations. This result underscored its limitations under nonlinear dynamics. On the other hand, the SMC provides strong robustness against nonlinearities and uncertainties. It offers more reliable payload swing suppression despite slightly slower cart convergence. Under disturbance rejection tests, a disturbance of amplitude one was introduced at 6.5 seconds. The composite controller and SMC exhibited superior resilience, rapidly rejecting disturbances and restoring system stability. In contrast, PID responses were less robust and subject to extended oscillations. Furthermore, under system uncertainty with altered cart mass, payload mass and cable length, the composite controller maintained accurate tracking and effective swing suppression, while SMC preserved robustness, although with slower dynamics; PID performance deteriorated noticeably due to overshoot and increased oscillations. Collectively, the findings indicate that the composite controller offers the best trade-off between tracking precision and swing suppression. SMC ensures robustness to uncertainties and disturbances and PID provides simplicity and fast response at the expense of reduced robustness. These results highlight the importance of the composite control strategies in ensuring safe and efficient operation of underactuated crane systems subject to uncertainty and external disturbances. This study is limited to simulation-based evaluation. Future work may focus on experimental validation and extension to three-dimensional crane motion.

Conflict of Interest

The authors have no conflict of relevant interest to this article.

References

[1] Z. Zhang, J. Liu, and Y. Zhang, “Design of anti-swing PID controller for bridge crane based on PSO and SA algorithm.” Electronics, vol. 11, no. 19, Article 3143, 2022. https://doi.org/10.3390/electronics11193143

[2] K. Kayışlı, ans M. Uğur, “Fuzzy logic and PID control of a 3 DOF robotic arm.” Gazi Üniversitesi Fen Bilimleri

Dergisi Part C: Tasarım ve Teknoloji, vol. 5, no. 4, pp. 223–233, 2017. https://doi.org/10.29109/http-gujsc-gazi-edu-tr.339907

[3] S. Milovanovic, M. M. Mladenovic, N. M. Nikolic, et al, "Optimal PID and fuzzy logic-based position controller design of an overhead crane using the Bees Algorithm." Discover Applied Sciences, vol. 1, Issue 5, 2021. https://doi.org/10.1007/s42452-021-04793-0

[4] J. Xu, C. Zhao, T. Wang, and L. Huang, "Research on anti-swing control system of slewing crane based on fuzzy PID." PLOS ONE, vol. 19, no. 10, 2024. https://doi.org/10.1371/journal.pone.0311701

[5] C. O. Azeloglu, A. Sagırlı, H. Yazıcı, and R. Guclu, "Gantry crane structure seismic control by the use of fuzzy PID controller." Gazi University Journal of Science, vol. 26, no. 2, pp. 215–223, 2013.

[6] X. Shao, X. Zhang, Q. Wang, and L. Chen, "A novel anti-swing and position control method for overhead crane." Advances in Mechanical Engineering, vol. 11, no. 3, 2019. https://doi.org/10.1177/0036850419883539

[7] E. H. Çopur, H. H. Bilgiç, and T. Ünler, "Artificial intelligence based LQR and PID controller design of 3 degree of freedom system." Necmettin Erbakan Üniversitesi Fen ve Mühendislik Bilimleri Dergisi, vol. 6, no. 3, pp. 457–467, 2024. https://doi.org/10.47112/neufmbd.2024.58

[8] T. Wen, Y. Fang, and B. Lu, "Neural network-based adaptive sliding mode control for underactuated dual overhead cranes suffering from matched and unmatched disturbances." Autonomous Intelligent Systems, vol. 2, no. 1, 2022. https://doi.org/10.1007/s43684-021-00019-7

[9] H. Y. Qiang, L. Zhang, J. Liu, and Y. Li, "Anti-sway and positioning adaptive control of a double-pendulum overhead crane system with neural network compensation." Frontiers in Robotics and AI, vol. 8, Article 639734, 2021. https://doi.org/10.3389/frobt.2021.639734

[10] H. Yıldız, "Computer aided simulation and PID control of a small scale single DOF magnetic pendulum mechanism." Journal of Engineering Sciences and Design, vol. 12, no. 1, pp. 75–87, 2024. https://doi.org/10.21923/jesd.1318257

[11] W. Tang, R. Ma, H. Jiang, et al., "Composite control design for double-pendulum overhead cranes." Meccanica, vol. 60, pp. 891–909, 2025. https://doi.org/10.1007/s11012-025-01961-z

[12] P. Kumar, S. Singh, and A. Verma, "Load shape-agnostic adaptive control for four-DOF overhead crane robots." Nonlinear Dynamics, vol. 111, pp. 2345–2362, 2025. https://doi.org/10.1007/s11071-025-11631-0

[13] M. Mohd Annuar, N. A. Ab. Halim, S. N. S. Mirin, and A. H. Azahar, "Dynamic modelling and analysis of 3D overhead gantry crane system." International Journal of Engineering & Technology, vol. 7, no. 3, pp. 1257–1262, 2018. https://doi.org/10.14419/ijet.v7i3.10099

[14] Y. Zhang, W. Chen, and X. Liu, "Position-commanding anti-sway controller for 2-D overhead cranes under velocity and acceleration constraints." IEEE Transactions on Industrial Electronics, vol. 70, no. 4, pp. 3205–3215, 2023. https://doi.org/10.1109/ACCESS.2023.3265586